

Landau-Pomeranchuk-Migdal effect for finite targets

Richard Blankenbecler and Sidney D. Drell

Stanford Linear Accelerator Center, Stanford University, Stanford, California 94309

(Received 2 October 1995)

In this paper the high-energy expansion for scattering from extended targets that the authors previously applied to beamstrahlung radiation and pair production is applied to the problem of radiation in a medium with multiple scattering. The suppression of the emission of long-wavelength photons, the Landau-Pomeranchuk-Migdal effect, is treated and explained in physical terms. This treatment of single-photon emission extends previous classical treatments of the problem to the quantum domain and corrects certain approximations made in these earlier works. The effects of finite target thickness is treated. A quantum treatment of multiple scattering is also given to aid in the physical interpretation of the suppression effect and to completely define our model of multiple scattering. [S0556-2821(96)01211-8]

PACS number(s): 41.60.-m, 13.40.-f, 11.80.Fv

I. INTRODUCTION AND MOTIVATION

Perhaps the most ubiquitous process in high-energy physics is the bremsstrahlung of photons by a charged particle in the field of an atom first described by Bethe and Heitler [1]. Following the experimental confirmation in 1993 of the Landau-Pomeranchuk-Migdal (LPM) effect [2–5], there is renewed interest in extensions of this process as well as its strong interaction analogue, gluon radiation at very high energies in heavy nuclei. In this paper we describe the application of eikonal techniques developed for the beamstrahlung process [6] that lead to a simpler, more straightforward, and physically transparent quantum-mechanical derivation of the LPM suppression of soft-photon radiation from high-energy electrons in dense matter. This exposition fills in some of the important steps omitted in our recent preprint [7] and extends the treatment in two ways. We analyze more fully our model of the random-scattering medium, and we also analyze the effects of finite-target thickness for comparison with the recent data.

This effect was first described by Landau and Pomeranchuk [8], who treated the classical radiation of a high-energy particle in the fluctuating and random field inside an infinitely thick medium. The minimum longitudinal-momentum transfer, q_{\parallel} , by a high-energy electron of momentum p and mass m , radiating a photon of momentum $k \equiv (1-x)p$, is given by $q_{\parallel}^{\min} = m^2(1-x)/2xp$. The uncertainty principle is used to define the formation length $l_f = (1/q_{\parallel}^{\min})$, which at high energies ($p \gg m$) and soft-photon emission ($1-x \ll 1$) can become large relative to the scattering mean free path of the electron. When this occurs, coherence is lost, leading to suppression of the radiation.

In their classical derivation, which is appropriate to this kinematic limit, $k \ll p$, Landau and Pomeranchuk were the first to show that the familiar Bethe-Heitler radiated photon spectrum, $dN \sim dk/k$, is modified by the multiple scattering of the electron as it traverses the rapidly varying electric fields of the medium. When the mean free path of the electron, αL , is comparable to or less than the formation length l_f , they found that the spectrum is suppressed, ultimately achieving the form

$$dN \sim dk/(p\sqrt{Lk}). \quad (1.1)$$

Subsequently, Migdal [9] presented a quantum-mechanical derivation of this effect, treating multiple scattering via the Vlasov equation and including the effects of electron spin and energy loss. His derivation contains a number of approximations that are formally difficult, not very transparent on physical grounds, and numerically not well controlled. These works have been extended by several authors [10].

The approach presented here is a simple application of the eikonal formalism previously developed for high-energy beamstrahlung processes and has the advantage of greater generality and physical transparency. Aside from providing a simple and intuitive framework for more accurate studies of the LPM effect, including finite target thickness, our motivation is to provide a formalism that may be adapted to other problems such as radiation by electrons transiting random magnetic domains and non-Abelian gluon radiation by quarks transiting heavy nuclei and undergoing multiple inelastic collisions [11,12].

As described earlier, the essential physics used in LPM leading to the behavior in (1.1) is the random scattering of the electron while transiting matter. The radiation length L is energy independent at high energy, being given for screened Coulomb fields by

$$\frac{1}{L} = 4n\alpha r_e^2 Z^2 \ln(183/Z^{1/3}), \quad (1.2)$$

where $r_e = \alpha/m = 2.8$ fm and n is the number density of target particles. The mean free path is defined as αL . In traversing a path length z , the longitudinal momentum transfer due to multiple scattering of the electron increases to

$$q_z = \left(E - \frac{m^2 + (\delta\vec{p}_{\perp})^2}{2p} \right) - \left(k + xE - \frac{m^2 + (\delta\vec{p}_{\perp})^2}{2xp} \right) \\ = \frac{k}{2xp^2} [m^2 + (\delta\vec{p}_{\perp})^2], \quad (1.3)$$

where the classically calculated, mean-square, transverse momentum transfer is given by

$$(\delta\vec{p}_\perp)^2 \sim \left| \int_0^{(1/2)z} dz' \vec{E}_\perp(z') \right|^2. \quad (1.4)$$

$\vec{E}_\perp(z')$ is the random (from one electron to the next) atomic electric field that scatters the electron over its path length of $(1/2)z$, the average for both the incident and scattered electron; higher-order effects, such as scattering of the photon by the medium, are neglected [13]. The standard formula for multiple scattering by statistically independent atoms is [14]

$$(\delta\vec{p}_\perp)^2 = \frac{E_s^2}{L} \left(\frac{1}{2} z \right), \quad E_s^2 = \frac{4\pi m^2}{\alpha} \sim (21 \text{ MeV})^2. \quad (1.5)$$

Identifying $q_{\text{ms}} \sim 1/z$ by the uncertainty principle, we obtain from (1.3)

$$z \sim l_f \left(1 + \frac{E_s^2}{2m^2 L} z \right)^{-1}, \quad (1.6)$$

so that in the Bethe-Heitler limit of no multiple scattering, $z_{\text{BH}} \sim l_f \propto 1/k$, whereas for strong multiple scattering, $z_{\text{LPM}} \sim \sqrt{l_f} \propto 1/\sqrt{k}$.

This simple argument, confirming (1.1), indicates that the $1/p$ corrections are necessary in the eikonal treatment. As emphasized in [6] the zeroth-order eikonal approximation treats straight-line propagation through the medium in the limit of zero transfer of longitudinal momentum, $q_z \rightarrow 0$. In contrast, here the multiple-scattering corrections to a finite $q_z \sim 1/p$ are of interest, as shown in (1.3). Let us now turn to some details of the formulation and calculation.

II. EIKONAL TREATMENT

We review here the eikonal formulation for high-energy scattering by the static fields of a medium at rest; for more details, see [6]. For simplicity [15] we consider the Klein-Gordon equation for a scalar particle of mass m in a static external field, which can be written

$$[(E - V)^2 + \vec{\nabla}^2 - m^2] \phi(\vec{r}) = 0, \quad (2.1)$$

and write the scattering potential in cylindrical coordinates,

$$V(r) = V(z, \vec{b}_\perp), \quad \vec{b}_\perp^2 = x^2 + y^2. \quad (2.2)$$

We look for solutions satisfying the requisite initial and final (outgoing and incoming) boundary conditions. The solution will be written in the form

$$\phi(\vec{r}) = \exp[i\Phi(\vec{r})], \quad (2.3)$$

where the phase function Φ satisfies the equation

$$(E - V)^2 - m^2 = [\vec{\nabla}\Phi(\vec{r})]^2 - i\vec{\nabla}^2\Phi(\vec{r}). \quad (2.4)$$

For the incident wave, the leading term in Φ_i will be $p^i z$ for the incident particle momentum along the z axis. The phase function to order $(1/p^i)$ for initial (outgoing) scattering boundary conditions is written

$$\Phi^i = p^i z - \chi_0(z, \vec{b}_\perp) - \frac{1}{p^i} [\chi_1(z, \vec{b}_\perp) + i\chi_2(z, \vec{b}_\perp)]. \quad (2.5)$$

Substitution into (2.4) then yields

$$\chi_0(z, \vec{b}_\perp) = \int_{-\infty}^z dz' V(z', \vec{b}_\perp), \quad (2.6)$$

which is recognized as the usual eikonal form. The leading $(1/p)$ corrections are (for p_\perp^i not zero)

$$\begin{aligned} \chi_1(z, \vec{b}_\perp) &= \frac{1}{2} \int_{-\infty}^z dz' [[\vec{\nabla}_\perp \chi_0(z', \vec{b}_\perp)]^2 \\ &\quad - 2\vec{p}_\perp^i \cdot \vec{\nabla}_\perp \chi_0(z', \vec{b}_\perp)], \\ \chi_2(z, \vec{b}_\perp) &= \frac{1}{2} \int_{-\infty}^z dz' [\vec{\nabla}^2 \chi_0(z', \vec{b}_\perp)]. \end{aligned} \quad (2.7)$$

For the final state with incoming-wave boundary conditions, the leading term in Φ_f must contain the final electron momentum written as $\vec{p}^f = (z p^f + \vec{b} p_\perp^f)$. The phase function to order $(1/p^f)$ will be written as

$$\Phi^f = \vec{p}^f \cdot \vec{r} + \tau_0(z, \vec{b}_\perp) + \frac{1}{p^f} [\tau_1(z, \vec{b}_\perp) + i\tau_2(z, \vec{b}_\perp)], \quad (2.8)$$

and then substitution into (2.4) yields the solution

$$\tau_0(z, \vec{b}_\perp) = \int_z^\infty dz' V(z', \vec{b}_\perp), \quad (2.9)$$

which is again in the familiar eikonal form, and the leading corrections in this case are

$$\begin{aligned} \tau_1(z, \vec{b}_\perp) &= \frac{1}{2} \int_z^\infty dz' [[\vec{\nabla}_\perp \tau_0(z', \vec{b}_\perp)]^2 + 2\vec{p}_\perp^f \cdot \vec{\nabla}_\perp \tau_0(z', \vec{b}_\perp)] \\ \tau_2(z, \vec{b}_\perp) &= \frac{1}{2} \int_z^\infty dz' [\vec{\nabla}^2 \tau_0(z', \vec{b}_\perp)]. \end{aligned} \quad (2.10)$$

The total phase appearing in the bremsstrahlung matrix element also includes the phase [16] of the photon wave function $A(\vec{r})$. Defining the momentum transfer to the medium as $\vec{q} = \vec{p}^f + \vec{k} - \vec{p}^i$, the total phase can be written in the form

$$\begin{aligned} \Phi^{\text{tot}} &= \Phi^i - \Phi^f - \vec{k} \cdot \vec{r} \\ &= -\vec{q} \cdot \vec{r} - \chi_0^{\text{tot}}(\vec{b}_\perp) - \frac{1}{p} [\chi_1^{\text{tot}}(z, \vec{b}_\perp) + i\chi_2^{\text{tot}}(z, \vec{b}_\perp)], \end{aligned} \quad (2.11)$$

where from now on $p \equiv p^i$, and total phase functions have been introduced as the appropriate sum of a χ and a τ . Therefore the zeroth-order term is independent of z

$$\chi_0^{\text{tot}}(\vec{b}_\perp) = \int_{-\infty}^\infty dz' V(z', \vec{b}_\perp), \quad (2.12)$$

while the first-order terms still retain some z dependence:

$$\begin{aligned}\chi_1^{\text{tot}}(z, \vec{b}_\perp) &= \chi_1(z, \vec{b}_\perp) + \frac{1}{x} \tau_1(z, \vec{b}_\perp), \\ \chi_2^{\text{tot}}(z, \vec{b}_\perp) &= \chi_2(z, \vec{b}_\perp) + \frac{1}{x} \tau_2(z, \vec{b}_\perp),\end{aligned}\quad (2.13)$$

where, as defined earlier, $x = p^f/p^i$. The term χ_1^{tot} is crucial in a proper description of both multiple scattering and the LPM process. It represents a leading correction to the z dependence of the total phase, since as we saw in (1.3), q_z is also of order $1/p$. However, there is no need to retain the $1/p$ corrections to the amplitude at high energies. Therefore the term χ_2^{tot} , which describes the amplitude change of the wave functions, can be neglected as unimportant in this application.

III. MODEL OF THE RANDOM MEDIUM

To define a model for the medium, we use the fact that the eikonal phase, as shown in Eqs. (2.6)–(2.13), involves longitudinal-line integrals through the target. As the electron traverses the target, it will be subject to accelerations due to the electric fields of the individual nearby atoms that it passes.

The simplest model of a random medium incorporates the physical assumption that the sum of transverse fields along any segment of the particle's trajectory that includes many atoms—i.e., when the segment is long compared with the interatomic spacing—is independent of \vec{b}_\perp , the particle's impact parameter in the medium. Therefore, in this model the $1/p$ terms in the eikonal phase that record the transverse momenta transferred to the particle depend only on the path length z :

$$\chi_1(z, \vec{b}_\perp) = \chi_1(z) \quad \text{and} \quad \tau_1(z, \vec{b}_\perp) = \tau_1(z). \quad (3.1)$$

Consistent with this assumption, we set

$$V(z, \vec{b}_\perp) = -\vec{b}_\perp \cdot \vec{E}_\perp(z). \quad (3.2)$$

The transverse field varies with depth z from atom to atom. The quantity $\vec{E}_\perp(z)dz$ is the differential transverse momentum acquired in traversing from z to $z+dz$. Its fluctuating nature, from one incident particle to the next, is expressed by the statistical, or ensemble, average given by

$$\langle \vec{E}_\perp(z_2) \cdot \vec{E}_\perp(z_1) \rangle = \frac{\langle \vec{p}_\perp^2 \rangle}{L} \delta(z_2 - z_1), \quad (3.3)$$

in the absence of correlations between fields at different depths. In Eq. (3.3) $\langle \vec{p}_\perp^2 \rangle$ is the average transverse momentum accumulated via multiple scattering in traversing a radiation length L . This relation, independent of b , allows one to compute all the statistical averages that will be needed in the following discussion. This is a quantum version of the classical model introduced by Landau and Pomeranchuk [8] in their original paper.

A simple physical description can be given of this model of the scattering along the trajectory of the projectile by approximating the screened Coulomb potentials by a Gaussian

potential. In this case, the δ function in Eq. (3.3) is replaced by $C(z_2 - z_1) = (a\sqrt{2\pi})^{-1} \exp\{-(z_2 - z_1)^2/2a^2\}$, where a is the range of the potential. For all but the lightest nuclei the screening radius a is much smaller than the interatomic spacing, and $C(z_2 - z_1) \rightarrow \delta(z_2 - z_1)$.

For notational clarity we define the integrals

$$\begin{aligned}\vec{A}_\perp^i(z) &= -\vec{\nabla}_\perp \chi_0(z, \vec{b}_\perp) = \int_{-\infty}^z dz' \vec{E}_\perp(z'), \\ \vec{A}_\perp^f(z) &= -\vec{\nabla}_\perp \tau_0(z, \vec{b}_\perp) = \int_z^\infty dz' \vec{E}_\perp(z'),\end{aligned}\quad (3.4)$$

$$\vec{A}_\perp = \int_{-\infty}^\infty dz' \vec{E}_\perp(z'), \quad \vec{A}_\perp(z_2, z_1) = \int_{z_1}^{z_2} dz' \vec{E}_\perp(z').$$

The quantity $\vec{A}_\perp(z_2, z_1)$ evidently represents the total transverse momentum accumulated in going from the point z_1 to the point z_2 in the target.

The zeroth-order phases can be written as

$$\begin{aligned}\chi_0(z, \vec{b}_\perp) &= -\vec{b}_\perp \cdot \vec{A}_\perp^i(z), \quad \tau_0(z, \vec{b}_\perp) = -\vec{b}_\perp \cdot \vec{A}_\perp^f(z), \\ \chi_0^{\text{tot}}(\vec{b}_\perp) &= -\vec{b}_\perp \cdot \vec{A}_\perp,\end{aligned}\quad (3.5)$$

where $\chi_0^{\text{tot}}(\vec{b}_\perp)$ depends only on \vec{b}_\perp . On the other hand, the real first-order correction terms depend only upon z in this model:

$$\begin{aligned}\chi_1(z) &= \frac{1}{2} \int_{-\infty}^z dz' [\vec{A}_\perp^i(z') \cdot \vec{A}_\perp^i(z')], \\ \tau_1(z) &= \frac{1}{2} \int_z^\infty dz' [\vec{A}_\perp^f(z') \cdot \vec{A}_\perp^f(z') - 2\vec{p}_\perp^f \cdot \vec{A}_\perp^f(z')],\end{aligned}\quad (3.6)$$

$$\chi_1^{\text{tot}}(z) = \chi_1(z) + \frac{1}{x} \tau_1(z).$$

IV. MULTIPLE SCATTERING

In this section we consider the propagation of a wave packet through the scattering medium in order to develop a geometric picture that confirms the interpretation we gave to \vec{A}_\perp as the net transverse momentum acquired by the particle in traversing the medium.

We assume an incident plane-wave packet of the form

$$\phi_0(r, t) = \int \frac{d^3p}{(2\pi)^3} \langle \vec{p}, \vec{p}^i \rangle \exp\{i[\vec{p} \cdot \vec{r} - E(p)t]\}, \quad (4.1)$$

where $\langle \vec{p}, \vec{p}^i \rangle$ is a normalized Gaussian packet of width w :

$$\langle \vec{p}, \vec{p}^i \rangle = N \exp[-w^2(\vec{p} - \vec{p}^i)^2], \quad (4.2)$$

with N the normalization constant. Expanding $E(p)$ to linear terms in $(\vec{p} - \vec{p}^i)$, the incident packet becomes

$$\phi_0(r, t) = \exp\{i[\vec{p}^i \cdot \vec{r} - E_i t]\} \exp[-(\vec{r} - \vec{v}^i t)^2/(4w^2)], \quad (4.3)$$

where $\vec{v}^i = (v^i, 0_\perp)$ is the incident packet velocity and $E_i = E(p_i)$. Thus the packet probability distribution is

$$|\phi_0(r, t)|^2 = \exp[-(\vec{r} - \vec{v}^i t)^2 / (2w^2)]. \quad (4.4)$$

We consider a particle traversing a medium extending from $z=0$ to l in which the scatterers are randomly placed, and calculate the eikonal phase of its wave function $\phi(r, t)$ as defined in Eqs. (2.5) and (3.1). For ($z < 0$), there are no interactions and the phase is $\vec{p}^i \cdot \vec{r}$. Inside the medium ($0 \leq z \leq l$), the phase changes as a function of z as the particle trajectory encounters additional scatterers. On the far side on the medium, ($z > l$), beyond the range of any potential, the phase integrals saturate and remain constant:

$$\chi_0(l, \vec{b}_\perp) = \int_0^l dz' V(z', \vec{b}_\perp)$$

and

$$\vec{A}_\perp(l) = -\vec{\nabla}_\perp \chi_0(l, \vec{b}_\perp), \quad (4.5)$$

$$\chi_1^\zeta(z) = (z-l) \frac{1}{2} \vec{A}_\perp(l) \cdot \vec{A}_\perp(l) + \chi_1^\zeta(l), \quad (4.6)$$

$$\vec{\chi}_1^\perp(z) = (z-l) \vec{A}_\perp(l) + \vec{\chi}_1^\perp(l),$$

where the two terms in Eq. (2.7) are

$$\chi_1^\zeta(l) = \frac{1}{2} \int_0^l dz' \vec{A}_\perp^i(z') \cdot \vec{A}_\perp^i(z'), \quad \vec{\chi}_1^\perp(l) = \int_0^l dz' \vec{A}_\perp^i(z'). \quad (4.7)$$

Expanding the phase function to first order around the central value of the packet momentum, $\vec{p}^i = (p^i, 0_\perp)$, one gets

$$\Phi - \Phi^i = (\vec{p} - \vec{p}^i) \cdot \vec{R}(z, \vec{b}_\perp),$$

where

$$R_z(z) = z + \frac{1}{2(p^i)^2} \left[(z-l) \vec{A}_\perp^2(l) + \int_0^l dz' \vec{A}_\perp^i(z') \cdot \vec{A}_\perp^i(z') \right],$$

$$\vec{R}_\perp(z, \vec{b}_\perp) = \vec{b}_\perp - \frac{1}{p^i} \left[(z-l) \vec{A}_\perp(l) + \int_0^l dz' \vec{A}_\perp^i(z') \right]. \quad (4.8)$$

Therefore, the probability distribution of the wave packet after emerging from the medium is

$$|\phi(r, t)|^2 = \exp[-[R(z, \vec{b}_\perp) - \vec{v}^i t]^2 / (2w^2)]. \quad (4.9)$$

Introducing (Z, \vec{B}_\perp) as the coordinates of the center of the packet and T_l as the time the packet emerges from the medium, one finds from (4.8) that

$$v^i T_l = l + \frac{1}{2(p^i)^2} \int_0^l dz' \vec{A}_\perp^i(z') \cdot \vec{A}_\perp^i(z') \quad (4.10)$$

and

$$(Z-l) = \frac{v^i}{[1 + [1/2(p^i)^2] \vec{A}_\perp^2(l)]} (t - T_l).$$

After passing through the medium, the packet moves linearly with time with a reduced z component of velocity, and it is therefore compelling to identify the angle of deviation of the particle θ , as

$$\cos(\theta) = \frac{1}{[1 + [1/2(p^i)^2] \vec{A}_\perp^2(l)]}, \quad (4.11)$$

or $\theta^2 \sim [\vec{A}_\perp(l)/p^i]^2$. This is in agreement with the interpretation of \vec{A}_\perp as the net transverse momentum acquired by the particle in traversing the medium, and is consistent with (3.3).

The transverse position of the center of the packet also tracks the longitudinal position,

$$\vec{B}_\perp = \frac{1}{p^i} \left((Z-l) \vec{A}_\perp(l) + \int_0^l dz' \vec{A}_\perp^i(z') \right). \quad (4.12)$$

The center of the packet moves at an angle τ with respect to the incident direction, where to order $1/p^i$, $\sin(\theta) \sim |\vec{A}_\perp(l)|/p^i$.

Using Eq. (3.3) to perform the ensemble averages over the packet probability distribution for multiple scattering through the random medium, we find to the inherent accuracy of our eikonal wave function and as expected from Eq. (4.11):

$$(p^i)^2 \langle \theta^2 \rangle = \langle \vec{A}_\perp^2(l) \rangle = \int_0^l dz \int_0^l dz' \langle \vec{E}_\perp(z) \cdot \vec{E}_\perp(z') \rangle$$

or

$$\langle \theta^2 \rangle = \frac{\langle \vec{p}_\perp^2 \rangle}{(p^i)^2} \frac{l}{L}. \quad (4.13)$$

The average transit time also shows quadratic growth with the thickness

$$v^i \langle T_l \rangle = 1 + \frac{1}{2(p^i)^2} \int_0^l dz' \langle \vec{A}_\perp^i(z', \vec{b}_\perp) \cdot \vec{A}_\perp^i(z', \vec{b}_\perp) \rangle$$

$$= l \left[1 + \frac{\langle \vec{p}_\perp^2 \rangle}{4(p^i)^2} \frac{l}{L} \right]. \quad (4.14)$$

As the statistically averaged packet exits from the target it is centered about the same value of \vec{b}_\perp as was the incident packet. However, the square of the packet width w^2 is increased. The mean-square width of the packet when it emerges from the medium at the point $z=l$ is therefore

$$w^2 + \langle B^2 \rangle = w^2 + \langle \theta^2 \rangle \frac{l^3}{3L}. \quad (4.15)$$

For large times, one finds that the root-mean-square width of the transmitted packet increases as z , which in turn grows linearly in t .

V. BREMSSTRAHLUNG IN A FIXED FIELD

We turn now to a derivation of single-photon emission by a spinless electron traversing the target medium. At a later appropriate point, the extension to the case of Dirac electrons will be made. The simplified model of the medium introduced in Sec. III, Eq. (3.2), will be assumed.

The general form of the matrix element of interest is

$$M = \langle \phi_f^{(-)} | \vec{A} \cdot \vec{J} - A_0 J_0 | \phi_i^{(+)} \rangle, \quad (5.1)$$

where $\vec{J} \equiv ie(\vec{\nabla} - \vec{\nabla})$ is the electron current, and $\phi_f^{(-)}$ and $\phi_i^{(+)}$ are, respectively, the final (incoming) and initial (outgoing) scattering eigenstates of the electron in the static field of the target. The calculation will be carried out in the target rest frame.

For scalar electrons, the matrix element takes the form

$$M = ie \int dz \int d^2 b_{\perp} \exp[-ik \cdot \vec{r}] \{ \vec{\epsilon}^* \cdot [\phi_f^{(-)*} \vec{\nabla} \phi_i^{(+)} - \phi_i^{(+)} \vec{\nabla} \phi_f^{(-)*}] - i \epsilon_0^* [E_i + E_f - 2V(z, b)] \phi_f^{(-)*} \phi_i^{(+)} \}, \quad (5.2)$$

where \vec{k} is the momentum, $\vec{\epsilon}$ the polarization vector of the photon, and from gauge invariance, $\epsilon_0 = \vec{\epsilon} \cdot \vec{k} / k_0$ where $k_0 = E_i - E_f$. Gauge invariance is easily proven by replacing ϵ_{μ} by k_{μ} , replacing \vec{k} by a derivative acting on the photon wave function, and integrating by parts. The result is zero if the wave functions satisfy the Klein-Gordon equation. Using the eikonal forms (2.3) and (2.11), the matrix element can be written as

$$M = -e \int dz \int d^2 b_{\perp} \vec{\epsilon}^* \cdot \vec{P}(z, \vec{b}_{\perp}) \exp[i\Phi_{\text{tot}}(z, \vec{b}_{\perp})], \quad (5.3)$$

where the factor $\vec{P}(z, \vec{b}_{\perp})$ involves the sum of the initial and final local momentum at the point (z, \vec{b}_{\perp})

$$\vec{P}(z, \vec{b}_{\perp}) = \vec{\nabla}(\Phi_i + \Phi_f) - \frac{\vec{k}}{k_0} [E_i + E_f - 2V(z, \vec{b}_{\perp})]. \quad (5.4)$$

Using the earlier expressions given for the phase functions, the convection current is

$$\begin{aligned} \nabla_z(\Phi_i + \Phi_f) &= (1+x)p, \\ \nabla_{\perp}(\Phi_i + \Phi_f) &= \vec{p}_{\perp}^f + \vec{A}_{\perp}^i(z) - \vec{A}_{\perp}^f(z). \end{aligned} \quad (5.5)$$

Combining the previous formulas, we find

$$P_z(z, \vec{b}_{\perp}) = 0,$$

$$\vec{P}_{\perp}(z, \vec{b}_{\perp}) = -\frac{2}{(1-x)} [\vec{k}_{\perp} - (1-x)\vec{A}_{\perp}^i(z)] + [\vec{q}_{\perp} - \vec{A}_{\perp}], \quad (5.6)$$

$$\Phi^{\text{tot}}(z, \vec{b}_{\perp}) = -\vec{q} \cdot \vec{r} + \vec{b}_{\perp} \cdot \vec{A}_{\perp} - \frac{1}{p} \chi_1^{\text{tot}}(z),$$

where only terms of relevant leading order in $1/p$ were retained.

The z component of the difference vector $\vec{q} (= \vec{p}^f + \vec{k} - \vec{p}^i)$ is

$$\begin{aligned} -q_z &= \frac{m^2 + (\vec{p}_{\perp}^f)^2}{2xp} + \frac{(\vec{k}_{\perp})^2}{2(1-x)p} - \frac{m^2}{2p} \\ &= \frac{[m^2(1-x)^2 + x(\vec{k}_{\perp})^2 + (1-x)(\vec{p}_{\perp}^f)^2]}{2x(1-x)p}. \end{aligned} \quad (5.7)$$

Now the matrix element can be simplified by noting that the current $P(z, \vec{b}_{\perp})$ is actually independent of b in the model of Eq. (3.2) for the external field, and hence

$$M = -e(2\pi)^2 \delta(\vec{q}_{\perp} - \vec{A}_{\perp}) \int dz \vec{\epsilon}^* \cdot \vec{P}(z, 0) \exp[i\Phi_{\text{tot}}(z, 0)]. \quad (5.8)$$

Defining A to be the frontal area of the target, the square of the matrix element summed over polarization is

$$\sum_{\text{pol}} |M|^2 = 4\pi\alpha A (2\pi)^2 \delta(\vec{q}_{\perp} - \vec{A}_{\perp}) I$$

with

$$I = \int_{-\infty}^{\infty} dz_2 \int_{-\infty}^{\infty} dz_1 S_0(z_2, z_1) \exp\{i[\Phi_{\text{tot}}(z_2, 0) - \Phi_{\text{tot}}(z_1, 0)]\},$$

$$I = 2 \int_{-\infty}^{\infty} dz_2 \int_{-\infty}^{z_2} dz_1 S_0(z_2, z_1) \cos[\Delta\Phi_{\text{tot}}(z_2, z_1)],$$

$$S_0(z_2, z_1) = S_0(z_1, z_2) = \sum_{\text{pol}} \vec{\epsilon}^* \cdot \vec{P}(z_2, 0) \vec{\epsilon} \cdot \vec{P}(z_1, 0). \quad (5.9)$$

The phase difference is written as

$$\Delta\Phi_{\text{tot}}(z_2, z_1) = \int_{z_1}^{z_2} dz \frac{d\Phi_{\text{tot}}(z, 0)}{dz}, \quad (5.10)$$

where

$$\frac{d\Phi_{\text{tot}}(z, 0)}{dz} = -q_z - \frac{1}{p} \frac{d\chi_1^{\text{tot}}(z)}{dz}.$$

Eliminating \vec{A}_\perp^f in this expression in favor of \vec{A}_\perp^i and $\vec{A}_\perp (= \vec{q}_\perp)$ by (5.8), and using the explicit expression (5.7) for q_z , this quantity simplifies to

$$\frac{d\Phi_{\text{tot}}(z, 0)}{dz} = \frac{1}{2x(1-x)p} \{m^2(1-x)^2 + [\vec{k}_\perp - (1-x)(\vec{A}_\perp^i(z))]^2\}, \quad (5.11)$$

where the transverse momentum dependence of the photon is measured relative to the modulated path of the electron as it moves through the medium.

Since $\vec{\epsilon}$ is orthogonal to \vec{k} , the polarization sum is straightforward:

$$\begin{aligned} S_0(z_2, z_1) &= \vec{P}_\perp(z_2, 0) \cdot \vec{P}_\perp(z_1, 0) - \hat{k} \cdot \vec{P}_\perp(z_2, 0) \hat{k} \cdot \vec{P}_\perp(z_1, 0) \\ &= \vec{P}_\perp(z_2, 0) \cdot \vec{P}_\perp(z_1, 0) \\ &= \frac{4}{(1-x)^2} \{\vec{k}_\perp - (1-x)[\vec{A}_\perp^i(z_2)]\} \cdot \{\vec{k}_\perp - (1-x)[\vec{A}_\perp^i(z_1)]\}, \end{aligned} \quad (5.12)$$

where the relation $\vec{q}_\perp = \vec{A}_\perp$ has been used and terms of order $(1/p^2)$ have been dropped.

Here we also introduce the explicit corrections to the polarization sum for Dirac electrons. Following the details as given by Schroeder [17], we substitute $S(z_2, z_1)$ for $S_0(z_2, z_1)$, where

$$S_0(z_2, z_1) \rightarrow S(z_2, z_1) = \frac{1+x^2}{2x} S_0(z_2, z_1) + \frac{1}{4} \frac{2m^2(1-x)^2}{x}, \quad (5.13)$$

where the two terms correspond, respectively, to no-helicity flip and to helicity flip by the radiating electron. We also introduce the notation $r(x) = (1+x^2)/2x$ for later use.

The probability that an electron incident upon the target will emit a photon of energy $k = (1-x)p$ is

$$\begin{aligned} \frac{dP(x)}{dx} &= \frac{1}{A} \frac{d\sigma}{dx} = \frac{1}{16\pi A p^2 x(1-x)} \int \frac{d^2 k_\perp}{(2\pi)^2} \int \frac{d^2 q_\perp}{(2\pi)^2} \sum_{\text{pol}} |M|^2 \\ &= \frac{\alpha}{2p^2 x(1-x)} \int \frac{d^2 k_\perp}{(2\pi)^2} \int_{-\infty}^{\infty} dz_2 \int_{-\infty}^{z_2} dz_1 S(z_2, z_1) \cos\left(\int_{z_1}^{z_2} dz \frac{d\Phi_{\text{tot}}(z, 0)}{dz}\right). \end{aligned} \quad (5.14)$$

Note that if there is no scattering in the target, then $S(z_2, z_1)$ does not depend upon the z 's and $d\Phi_{\text{tot}}(z, 0)/dz = \text{const}$. Thus the integrals over the z 's are zero; they yield δ functions that cannot be satisfied. It proves convenient to regulate (5.14) by subtracting this zero from the integrand. Later we will want to interchange the orders of integration to simplify the numerical evaluation. This will require care due to the infinite limits. By introducing suitable convergence factors we will show that the integrals smoothly approach their finite values as the convergence factors go to one. Thus the z integrals will be regulated by replacing dz by $dzC(z)$ where the cutoff function $C(z)$ is chosen to restrict integration to the physical region and to go smoothly to one after all integrations have been performed. The simplest choice is

$$C(z) = \exp(-\bar{\epsilon}|z|) \quad (5.15)$$

with

$$\frac{dC(z)}{dz} = -C(z)\bar{\epsilon}[\theta(z) - \theta(-z)] \equiv -C(z)\bar{\epsilon}\epsilon(z).$$

With the understanding that $\bar{\epsilon}$ will be taken to zero at the end of the calculation, the emission probability can now be written as

$$\frac{p(1-x)^2}{2\alpha} \frac{dP(x)}{dx} = \int \frac{d^2k_{\perp}}{(2\pi)^2} \int_{-\infty}^{\infty} dz_2 C(z_2) \int_{-\infty}^{z_2} dz_1 C(z_1) \Delta B(z_2, z_1),$$

$$\Delta B(z_2, z_1) = [B(z_2, z_1, \vec{k}_{\perp}) - B_0(z_2, z_1, \vec{k}_{\perp})], \quad (5.16)$$

where

$$B(z_2, z_1, \vec{k}_{\perp}) = r(x) \left(\frac{\partial}{\partial z_2} - \frac{\partial}{\partial z_1} \right) \sin[\Delta\Phi_{\text{tot}}(z_2, z_1)] - (1-x)^2 \frac{2m^2 + r(x)\vec{A}_{\perp}^2(z_2, z_1)}{2x(1-x)p} \cos[\Delta\Phi_{\text{tot}}(z_2, z_1)]. \quad (5.17)$$

$B_0(z_2, z_1, \vec{k}_{\perp})$ is the same expression in the limit of no interaction, $\vec{A}_{\perp}(z) = 0$. An integration by parts on z_1 and z_2 now leads to

$$B(z_2, z_1, \vec{k}_{\perp}) = \bar{\epsilon} r(x) [\epsilon(z_2) - \epsilon(z_1)] \sin[\Delta\Phi_{\text{tot}}(z_2, z_1)] - (1-x)^2 \frac{2m^2 + r(x)\vec{A}_{\perp}^2(z_2, z_1)}{2x(1-x)p} \cos[\Delta\Phi_{\text{tot}}(z_2, z_1)]. \quad (5.18)$$

Our problem now is to evaluate (5.16) with (5.18) in the physical situations of interest. First, however, we must confirm that the subtracted term, with B replaced by B_0 in (5.17), still vanishes and that we have not introduced a false contribution to the radiation probability by the choice of the convergence factor (5.15).

To examine this point, perform the integrals over z_1 and z_2 in the zero-field limit for the term involving

$$B_0(z_2, z_1, \vec{k}_{\perp}) = \bar{\epsilon} r(x) [\epsilon(z_2) - \epsilon(z_1)] \sin[\Delta\Phi_0(z_2, z_1)] - \frac{2m^2(1-x)^2}{2x(1-x)p} \cos[\Delta\Phi_0(z_2, z_1)], \quad (5.19)$$

where

$$\Delta\Phi_0(z_2, z_1) = \frac{z_2 - z_1}{2x(1-x)p} \{m^2(1-x)^2 + [\vec{k}_{\perp}]^2\}.$$

The last form follows from (5.15) and (5.17). The result is

$$\frac{p(1-x)^2}{2\alpha} \frac{dP_0(x)}{dx} \equiv \int \frac{d^2k_{\perp}}{(2\pi)^2} \left(\bar{\epsilon} I_1 - \frac{2m^2(1-x)^2}{2x(1-x)p} I_2 \right)$$

with

$$I_1 = \frac{4w\bar{\epsilon}}{(\bar{\epsilon}^2 + w^2)^2}, \quad I_2 = \frac{2\bar{\epsilon}^2}{(\bar{\epsilon}^2 + w^2)^2}, \quad (5.20)$$

and

$$w = \frac{m^2(1-x)^2 + \vec{k}_{\perp}^2}{2x(1-x)p}.$$

We obtain

$$\frac{p(1-x)^2}{2\alpha} \frac{dP_0(x)}{dx} \equiv \int \frac{d^2k_{\perp}}{(2\pi)^2} \frac{4\bar{\epsilon}^2}{(\bar{\epsilon}^2 + w^2)^2} \left[r(x)w - \frac{m^2(1-x)^2}{2x(1-x)p} \right]. \quad (5.21)$$

The integration over \vec{k}_{\perp} is well convergent and therefore the probability of emission vanishes as $\bar{\epsilon}$ goes to zero, as it must.

The regulated probability of radiation can now be written in the form

$$\frac{p(1-x)^2}{2\alpha} \frac{dP(x)}{dx} = \int \frac{d^2k_{\perp}}{(2\pi)^2} \int_{-\infty}^{\infty} dz_2 C(z_2) \int_{-\infty}^{z_2} dz_1 C(z_1) \Delta B(z_2, z_1, \vec{k}_{\perp}), \quad (5.22)$$

where the integrand has become

$$\Delta B(z_2, z_1, \vec{k}_{\perp}) = \bar{\epsilon} r(x) [\epsilon(z_2) - \epsilon(z_1)] \{ \sin[\Delta\Phi_{\text{tot}}(z_2, z_1)] - \sin[\Delta\Phi_0(z_2, z_1)] \} - \frac{2m^2(1-x)^2}{2x(1-x)p} \{ \cos[\Delta\Phi_{\text{tot}}(z_2, z_1)] - \cos[\Delta\Phi_0(z_2, z_1)] \} - \frac{(1-x)^2 r(x) \vec{A}_{\perp}^2(z_2, z_1)}{2x(1-x)p} \cos[\Delta\Phi_{\text{tot}}(z_2, z_1)]. \quad (5.23)$$

Equation (5.22) can be simplified further by defining

$$m^2 \eta(z_2, z_1, l) = \frac{1}{z_2 - z_1} \int_{z_1}^{z_2} dz [\vec{A}_\perp(z, z_1)]^2 - \left(\frac{1}{z_2 - z_1} \int_{z_1}^{z_2} dz \vec{A}_\perp(z, z_1) \right)^2,$$

and

$$m^2 \lambda(z_2, z_1, l) = \vec{A}_\perp^2(z_2, z_1). \quad (5.24)$$

Now we interchange the order of the integrals to do $\int d^2 \vec{k}_\perp$ first, and then shift the integration variable from \vec{k}_\perp to \vec{K}_\perp where

$$\vec{K}_\perp = \vec{k}_\perp - (1-x) \left(\vec{A}_\perp^i(z_1) + \frac{1}{z_2 - z_1} \int_{z_1}^{z_2} dz \vec{A}_\perp(z, z_1) \right). \quad (5.25)$$

The resulting expression is a function only of the magnitude \vec{K}_\perp^2 and we find for Eq. (5.22)

$$\frac{p(1-x)^2}{2\alpha} \frac{dP(x)}{dx} = \int_{-\infty}^{\infty} dz_2 \int_{-\infty}^{z_2} dz_1 C(z_2) C(z_1) \Delta B(z_2, z_1), \quad (5.26)$$

where

$$\begin{aligned} \Delta B(z_2, z_1) = & \int \frac{d^2 K_\perp}{(2\pi)^2} \left\{ \bar{\epsilon} r(x) [\epsilon(z_2) - \epsilon(z_1)] \{ \sin[\Delta(z_2, z_1, \vec{K}_\perp)] - \sin[\delta(z_2, z_1, \vec{K}_\perp)] \} - \frac{2m^2(1-x)^2}{2x(1-x)p} \right. \\ & \left. \times [\cos[\Delta(z_2, z_1, \vec{K}_\perp)] - \cos[\delta(z_2, z_1, \vec{K}_\perp)]] - \frac{r(x)m^2(1-x)^2 \lambda(z_2, z_1)}{2x(1-x)p} \cos[\Delta(z_2, z_1, \vec{K}_\perp)] \right\}, \quad (5.27) \end{aligned}$$

and

$$\Delta(z_2, z_1, \vec{K}_\perp) = \frac{z_2 - z_1}{2x(1-x)p} [m^2(1-x)^2 [1 + \eta(z_2, z_1, l)] + \vec{K}_\perp^2], \quad (5.28)$$

$$\delta(z_2, z_1, \vec{K}_\perp) = \frac{z_2 - z_1}{2x(1-x)p} [m^2(1-x)^2 + \vec{K}_\perp^2].$$

Using the (regulated) integrals

$$\int_0^\infty dy \cos(y) = 0, \quad \int_0^\infty dy y \cos(y) = -1, \quad (5.29)$$

$$\int_0^\infty dy \sin(y) = 1, \quad \int_0^\infty dy y \sin(y) = 0,$$

which were also regulated by setting $dy = dy C(y)$ and then taking the limit as $\bar{\epsilon}$ goes to zero, the integral over $y = \vec{K}_\perp^2$ can be performed. The result for the probability of emission is

$$\begin{aligned} \frac{\pi(1-x)}{\alpha x} \frac{dP(x)}{dx} = & \frac{m^2(1-x)}{xp} \int_{-\infty}^{\infty} dz_2 \int_{-\infty}^{z_2} dz_1 \frac{C(z_2) C(z_1)}{(z_2 - z_1)} \left[\left(1 + \frac{1}{2} r(x) \lambda(z_2, z_1, l) \right) \sin(c) - \sin(b) \right. \\ & \left. + \bar{\epsilon} \frac{xp r(x)}{m^2(1-x)} [\epsilon(z_2) - \epsilon(z_1)] [\cos(c) - \cos(b)] \right], \quad (5.30) \end{aligned}$$

where

$$\begin{aligned} c &= b [1 + \eta(z_2, z_1, l)], \\ b &= \frac{m^2(1-x)(z_2 - z_1)}{2xp}. \end{aligned} \quad (5.31)$$

Note that there is no singularity as $(z_2 - z_1)$ goes to zero. In all the examples that we shall discuss, the last term in the integrand vanishes smoothly in the limit as $\bar{\epsilon}$ goes to zero; this term can be safely dropped.

For later use, note that to first order in the square of the net impulse, A_\perp^2 , the probability of emission becomes

$$\frac{\pi(1-x)}{\alpha x} \left(\frac{dP(x)}{dx} \right)_1 = \frac{m^2(1-x)}{2xp} \int_{-\infty}^{\infty} dz_2 \int_{-\infty}^{z_2} dz_1 \frac{C(z_2)C(z_1)}{(z_2-z_1)} \{r(x)\lambda(z_2, z_1, l) \sin(b) + 2\eta(z_2, z_1, l)b \cos(b)\}. \quad (5.32)$$

This result holds for any fixed-field distribution in the target within our approximations. For a single (impulse) scattering, the probability of emission can be evaluated and compared to the Bethe-Heitler and to known classical formulas. Furthermore, if the fields in the target are averaged over, as is necessary in the multiple-scattering case, simplifications are also possible. These simplifications allow a direct comparison to the LPM result for very thick targets as well as an extension to the finite target-thickness case. These various limits are discussed in the next sections.

VI. THIN TARGET: SINGLE SCATTERING

As a first application we apply the lowest-order result, Eq. (5.32), to scattering by a thin target consisting of a single electric field slab, described by the potential function

$$V(z, b) = -\vec{b}_\perp \cdot \vec{Q}_\perp \delta(z)$$

and

$$\chi_0^{\text{tot}}(b) = -\vec{b}_\perp \cdot \vec{Q}_\perp, \quad (6.1)$$

where \vec{Q}_\perp is the total transverse momentum imparted by the field slab and clearly $l=0$. The phase integrals, (3.4), then become

$$\begin{aligned} \vec{A}_\perp^i(z) &= \vec{Q}_\perp \theta(z), & \vec{A}_\perp^f(z) &= \vec{Q}_\perp \theta(-z), \\ \vec{A}_\perp(z_2, z_1) &= \vec{Q}_\perp [\theta(z_2) - \theta(z_1)] = \vec{Q}_\perp \theta(z_2) \theta(-z_1). \end{aligned} \quad (6.2)$$

The first-order correction terms of interest depend upon z only, and Eq. (3.6) can be written simply for this case

$$\begin{aligned} \chi_1(z) &= \frac{1}{2} z \theta(z) [\vec{Q}_\perp^2], \\ \tau_1(z) &= -\frac{1}{2} z [\vec{Q}_\perp^2 - 2\vec{p}_\perp^f \cdot \vec{Q}_\perp], \\ \chi_1^{\text{tot}}(z) &= \chi_1(z) + \frac{1}{x} \tau_1(z). \end{aligned} \quad (6.3)$$

Two integrals that we will need are

$$\begin{aligned} \int_{z_1}^{z_2} dz \vec{A}_\perp(z, z_1) &= \vec{Q}_\perp z_2 \theta(z_2) \theta(-z_1), \\ \int_{z_1}^{z_2} dz [\vec{A}_\perp(z, z_1)]^2 &= \vec{Q}_\perp^2 z_2 \theta(z_2) \theta(-z_1). \end{aligned} \quad (6.4)$$

Thus we find

$$\begin{aligned} \lambda(z_2, z_1, 0) &= \frac{\vec{Q}_\perp^2}{m^2} \theta(z_2) \theta(-z_1), \\ \eta(z_2, z_1, 0) &= \lambda(z_2, z_1) \frac{-z_1 z_2}{(z_2 - z_1)^2}. \end{aligned} \quad (6.5)$$

Using (5.32), the probability of emission to lowest order in the impulse \vec{Q}_\perp and in the limit $\epsilon \rightarrow 0$, can be written as

$$\frac{\pi(1-x)}{\alpha x} \frac{dP(x)}{dx} = \frac{m^2(1-x)}{2xp} \int_{-\infty}^{\infty} dz_2 \int_{-\infty}^{z_2} dz_1 C(z_2)C(z_1) \frac{\lambda(z_2, z_1, 0)}{z_2 - z_1} \left(r(x) \sin(b) - \frac{2z_2 z_1 b}{(z_2 - z_1)^2} \cos(b) \right). \quad (6.6)$$

Now change variables to $b_i = z_i/l_f$ with $b = b_2 - b_1$. Recall that the formation length is given by

$$l_f = \frac{2xp}{m^2(1-x)}. \quad (6.7)$$

Interchange the orders of integration, use the explicit forms for $\eta(z_2, z_2 - z, 0)$ and $\lambda(z_2, z_2 - z, 0)$, and the probability of emission becomes

$$\frac{\pi(1-x)}{\alpha x} \frac{dP(x)}{dx} = \frac{\vec{Q}_\perp^2}{m^2} \int_0^\infty db \frac{C(b)}{b^2} I(b),$$

where

$$\begin{aligned} I(b) &= \int_0^b db_2 [r(x)b \sin(b) - 2b_2(b_2 - b) \cos(b)] \\ &= b^2 \left(r(x) \sin(b) + \frac{1}{3} b \cos(b) \right). \end{aligned} \quad (6.8)$$

The result of the final b integral is [see Eq. (5.29)]

$$\begin{aligned} (1-x) \frac{dP(x)}{dx} &= \frac{dI(\omega)}{d\omega} = \frac{\alpha}{\pi} \frac{\vec{Q}_\perp^2}{m^2} x \left(r(x) - \frac{1}{3} \right) \\ &= \frac{2}{3} \frac{\alpha}{\pi} \frac{\vec{Q}_\perp^2}{m^2} \left(x + \frac{3}{4} (1-x)^2 \right), \end{aligned} \quad (6.9)$$

where $I(\omega)$ is the radiated energy per unit-frequency interval at $\omega = p(1-x)$. If the appropriate value for the momentum transfer is used, this agrees with Bethe and Heitler.

In the $x \rightarrow 1$ limit this result can of course be simply obtained by a classical calculation. It is instructive to do this following the analysis of Landau and Pomeranchuk. Consider this thin-target example of a charged particle undergoing an instantaneous transverse impulse. Evaluate formula (1) and then the approximate formula (2) as given in their work [8]. As demonstrated in the Appendix, the result of the latter calculation is one-half that of the former. This is important for understanding the difference between their results and those we find from the eikonal method in both the Bethe-Heitler and in the LPM limits as shown in the following sections. The term omitted by LP gives rise to Cherenkov radiation under the appropriate conditions, i.e., when the dielectric constant is greater than $(E/p)^2$.

VII. FINITE-TARGET THICKNESS AND FIELD AVERAGING

Our next task is to manipulate Eq. (5.30) into a more convenient form in the case of a target of finite thickness. First note that the last term in the integrand leads to a finite integral; it can be safely dropped in the limit of vanishing $\bar{\epsilon}$. In the remaining terms it is convenient to change variables as in the previous section from z to $b = z/l_f$, where the inverse formation length was defined earlier. The radiation length L and the formation length l_f will play important roles in our result as will the scaled-target thickness $b_l = l/l_f$. The result for the probability of emission given in (5.30) can now be written as

$$\frac{\pi(1-x)}{\alpha x} \frac{dP(x)}{dx} = \int_{-\infty}^{\infty} db_2 \int_{-\infty}^{b_2} db_1 \frac{C(b_2)C(b_1)}{b} \left\{ \left(1 + \frac{r(x)\lambda(b_2, b_1, b_l)}{2(1-x)^2} \right) \sin(c) - \sin(b) \right\}, \quad (7.1)$$

where

$$c = b \left[1 + \frac{\eta(b_2, b_1, b_l)}{(1-x)^2} \right] \quad \text{and} \quad b = b_2 - b_1. \quad (7.2)$$

The target is assumed to extend from $0 < z < l$, or in terms of the scaled variables $0 < b < b_l$. The fact that the particles see no fluctuating field outside these limits requires that the integrals over the b 's in Eq. (7.1) be divided as follows:

$$\begin{aligned} \int_{-\infty}^{\infty} db_2 \int_{-\infty}^{b_2} db_1 &= \int_{-\infty}^0 db_2 \int_{-\infty}^{b_2} db_1 + \int_0^{b_l} db_2 \int_{-\infty}^0 db_1 \\ &+ \int_0^{b_l} db_2 \int_0^{b_2} db_1 + \int_{b_l}^{\infty} db_2 \int_{-\infty}^0 db_1 \\ &+ \int_{b_l}^{\infty} db_2 \int_0^{b_l} db_1 + \int_{b_l}^{\infty} db_2 \int_{b_l}^{b_2} db_1. \end{aligned} \quad (7.3)$$

In an obvious notation, these integration regions will be denoted by

$$\begin{aligned} \int_{-\infty}^{\infty} db_2 \int_{-\infty}^{b_2} db_1 &= (- -) + (0 -) + (00) + (+ -) + (+ 0) \\ &+ (+ +). \end{aligned} \quad (7.4)$$

The notation emphasizes the possible coherence between emission regions in the matrix element.

A. Statistical averages

The main formulas that we will need all arise from noting that the transverse electric field is zero outside the region $0 < z < l$ so that we may write

$$\vec{A}_{\perp}(z_2, z_1) = \int_{z_1}^{z_2} dz' \theta(z') \theta(l-z') \vec{E}_{\perp}(z'),$$

$$\int_{z_1}^{z_2} dz \vec{A}_{\perp}(z, z_1) = \int_{z_1}^{z_2} dz' \theta(z') \theta(l-z') \vec{E}_{\perp}(z') (z_2 - z'). \quad (7.5)$$

The statistical averages for the six integration regions can be computed directly from the above. Using Eq. (3.3) one finds in all integration regions that

$$\left\langle \int_{z_1}^{z_2} dz \vec{A}_{\perp}^2(z, z_1) \right\rangle = \left\langle \vec{A}_{\perp}(z_2, z_1) \cdot \int_{z_1}^{z_2} dz \vec{A}_{\perp}(z, z_1) \right\rangle = \frac{\langle \vec{p}_{\perp}^2 \rangle}{L} \int_{z_1}^{z_2} dz' \theta(z') \theta(l-z') (z_2 - z'), \quad (7.6)$$

$$\left\langle \left(\int_{z_1}^{z_2} dz \vec{A}_{\perp}(z, z_1) \right)^2 \right\rangle = \frac{\langle \vec{p}_{\perp}^2 \rangle}{L} \int_{z_1}^{z_2} dz' \theta(z') \theta(l-z') (z_2 - z')^2,$$

and

$$\langle \eta(z_2, z_1, l) \rangle = a \int_{z_1}^{z_2} dz' \theta(z') \theta(l-z') \frac{(z_2-z')(z'-z_1)}{(z_2-z_1)^2}, \quad \langle \lambda(z_2, z_1, l) \rangle = a \int_{z_1}^{z_2} dz' \theta(z') \theta(l-z'), \quad (7.7)$$

where

$$a = \frac{\langle p_{\perp}^2 \rangle}{m^2 L}.$$

or

$$\langle \lambda(b_2, b_1, b_l) \rangle = a l_f \int_{b_1}^{b_2} db' \theta(b') \theta(b_l - b').$$

In terms of scaled variables the other statistical average that we need is

After some algebra, the explicit results in the various regions in terms of the scaled variables are

Region	$\langle \eta(b_2, b_1, b_l) \rangle / 6(al_f)$	$\langle \lambda(b_2, b_1, b_l) \rangle / 1(al_f)$
(--)	0	0
(0-)	$\frac{b_2^2}{b^2} [3b - 2b_2]$	b_2
(+-)	$\frac{b_l}{b^2} [3(b_2 + b_1)b_l - 2b_l^2 - 6b_1b_2]$	b_l
(00)	b	b
(+0)	$\frac{(b_l - b_1)^2}{b^2} [3b - 2(b_l - b_1)]$	$(b_l - b_1)$
(++)	0	0

The interested reader can check that these formulas join smoothly at all common boundaries of the integration regions. Furthermore, the symmetry between (+) and (-), that is $(b_2 \leftrightarrow b_l - b_1)$, is also evident.

VIII. EMISSION PROBABILITY: BETHE-HEITLER REGIME

The probability of emission to lowest order, given in (5.32), is written as

$$\frac{\pi(1-x)}{\alpha x} \left(\frac{dP(x)}{dx} \right)_1 = a l_f \left(r(x) I_{\lambda} + \frac{1}{3} I_{\eta} \right),$$

where

$$I_{\lambda} = \int_{-\infty}^{\infty} db_2 \int_{-\infty}^{b_2} db_1 C(b_2) C(b_1) \frac{\lambda(b_2, b_1, b_l)}{a l_f} \frac{\sin(b)}{b} \quad (8.1)$$

and

$$I_{\eta} = \int_{-\infty}^{\infty} db_2 \int_{-\infty}^{b_2} db_1 C(b_2) C(b_1) \frac{6 \eta(b_2, b_1, b_l)}{a l_f} \cos(b).$$

All regions except (--) and (++) contribute to I_{λ} , and from symmetry $I_{\lambda}(+0) = I_{\lambda}(0-)$. Changing variables from db_1 to db , interchanging orders of integration, and performing the b_2 integral yields

$$I_{\lambda}(0-) = \frac{1}{2} \int_0^{b_l} db C(b) b \sin(b) + \frac{1}{2} b_l^2 \int_{b_l}^{\infty} db C(b) \frac{\sin(b)}{b},$$

$$I_{\lambda}(+-) = b_l \int_{b_l}^{\infty} db C(b) [b - b_l] \frac{\sin(b)}{b}, \quad (8.2)$$

$$I_{\lambda}(00) = \int_0^{b_l} db C(b) [b_l - b] \sin(b),$$

and

$$I_{\lambda}(\text{tot}) = b_l \int_0^{\infty} db C(b) \sin(b) = b_l.$$

The same regions contribute to I_{η} and again, $I_{\eta}(+0) = I_{\eta}(0-)$, so that

$$I_{\eta}(0-) = \frac{1}{2} \int_0^{b_l} db C(b) b^2 \cos(b) + \frac{1}{2} b_l^3 \int_{b_l}^{\infty} db \frac{C(b)}{b^2} [2b - b_l] \cos(b),$$

$$I_{\eta}(+-) = b_l \int_{b_l}^{\infty} db C(b) [b^3 - 2b_l^2 b + b_l^3] \frac{\cos(b)}{b^2}, \quad (8.3)$$

$$I_{\eta}(00) = \int_0^{b_l} db C(b) b [b_l - b] \cos(b),$$

and

$$I_{\eta}(\text{tot}) = b_l \int_0^{\infty} db C(b) b \cos(b) = -b_l.$$

The complete emission probability to linear order in a is therefore

$$\frac{\pi(1-x)}{\alpha x} \left(\frac{dP(x)}{dx} \right)_1 = a l_f b_l \left[r(x) - \frac{1}{3} \right]. \quad (8.4)$$

Since $l_f b_l = l$, the final result is

$$(1-x) \left(\frac{dP(x)}{dx} \right)_1 = \frac{2}{3} \frac{\alpha}{\pi} \frac{\langle \vec{p}_{\perp}^2 \rangle}{m^2} \frac{l}{L} \left[x + \frac{3}{4} (1-x)^2 \right]. \quad (8.5)$$

Note that (8.5) agrees with the thin-target result given earlier, Eq. (6.9), if one makes the obvious identification $\tilde{Q}_{\perp}^2 = \langle \vec{p}_{\perp}^2 \rangle l/L$.

Our model of multiple scattering is normalized by choosing $\langle \vec{p}_{\perp}^2 \rangle$ so that the emission probability agrees with the value quoted by Rossi [14] for incoherent multiple Coulomb scattering to leading order in a screened field:

$$(1-x) \left(\frac{dP(x)}{dx} \right)_1 = \frac{4}{3} \frac{l}{L} \left[x + \frac{3}{4} (1-x)^2 \right],$$

where

$$\langle \vec{p}_{\perp}^2 \rangle = \frac{2\pi m^2}{\alpha}. \quad (8.6)$$

In our model of multiple scattering, the average $\langle \vec{p}_{\perp}^2 \rangle$ acquired in each scattering event is smaller by a factor of 2 than the value given by Rossi for scattering in a screened Coulomb field. In their classical study of this same multiple-scattering model, Landau and Pomeranchuk were led to use the Rossi value by an error in their approximations that was discussed at the end of Sec. VI and is demonstrated explicitly in the Appendix. If their error is corrected, it is necessary to use Eq. (8.6) for this random-scattering model.

IX. EMISSION PROBABILITY: LPM REGIME

Recall that the probability of emission to all orders, given in (5.30), which includes the LPM effect, can be written in the form

$$\frac{\pi(1-x)}{\alpha x} \frac{dP(x)}{dx} = I(\text{tot}) = \int_{-\infty}^{\infty} db_2 \int_{-\infty}^{b_2} db_1 I(b_2, b_1, b_l), \quad (9.1)$$

where

$$I(b_2, b_1, b_l) = 2 \frac{C(b_2)C(b_1)}{b} \left\{ \left[1 + \frac{1}{2} r(x) \lambda(b_2, b_1, b_l) \right] \sin(c) - \sin(b) \right\}, \quad (9.2)$$

$$c = b [1 + \eta(b_2, b_1, b_l)],$$

and, of course, $b_i = z_i/l_f$ and $b = b_2 - b_1$. The integral $I(\text{tot})$ must be divided into all the subregions as defined in Eq. (7.3).

The regions $(-)$ and $(++)$ do not contribute since λ and η vanish. The first nonzero region is [recall that from symmetry, $I(0-) = I(+0)$]

$$I(0-) = \int_0^{b_l} db_2 \int_{-\infty}^0 db_1 I(0-; b_2, b_1, b_l) = \left[\int_0^{b_l} db \int_0^b db_2 + \int_{b_l}^{\infty} db \int_0^{b_l} db_2 \right] I(0-; b_2, b_2 - b, b_l), \quad (9.3)$$

where the $(0-)$ in the integrand indicates that λ and η are evaluated appropriately. The central region yields

$$I(00) = \int_0^{b_l} db_2 \int_0^{b_2} db_1 I(00; b_2, b_2 - b, b_l) = \int_0^{b_l} db \int_b^{b_l} db_2 I(00; b_2, b_2 - b, b_l) = \int_0^{b_l} db (b_l - b) I(00; b_2, b_2 - b, b_l), \quad (9.4)$$

since in this region neither λ nor η depend upon b_2 . The external region contributes:

$$I(+-) = \int_{b_l}^{\infty} db_2 \int_{-\infty}^0 db_1 I(+--; b_2, b_1, b_l) = \int_{b_l}^{\infty} db \int_{b_l}^b db_2 I(+--; b_2, b_2 - b, b_l). \quad (9.5)$$

A. Thick target

Let us now look at the (00) contribution to this amplitude, Eq. (9.4) and take the limit of large l . Using the results given in the quasitable in Sec. VII for $\langle \lambda \rangle$ and $\langle \eta \rangle$, we find

$$I(00) = \int_0^{b_l} db \frac{2C(b)}{b} (b_l - b) \left\{ \left(1 + \frac{1}{2} r(x) a l_f b \right) \sin \left(b + \frac{1}{6} a l_f b^2 \right) - \sin(b) \right\}, \quad (9.6)$$

where $C(b)$ can be set to one. In the limit of large l this result agrees with the form given by LP, however the formation length l_f is given correctly by Eq. (6.7) and the electron spin is properly accounted for by the factor $r(x)$. If $(1/6)al_f b_l \sim l/(\alpha L)$ is small compared to one, that is, if the target thickness is small compared to the mean free path, the LPM coherence vanishes since the phase behavior is essentially linear; this is the Bethe-Heitler regime. A direct expansion to order a of the above formula agrees with the result quoted in the previous section. As $al_f b_l$ becomes very large, which is the extreme LPM limit, only one term in (9.2) survives and it is of the order square root of a , that is,

$$\frac{\pi(1-x)}{\alpha x} \frac{dP(x)}{dx} \sim al_f \int_0^{b_l} db (b_l - b) \sin\left(b + \frac{1}{6} al_f b^2\right) r(x), \quad (9.7)$$

or

$$\begin{aligned} \frac{(1-x)}{l} \frac{dP(x)}{dx} &\sim \frac{axb_l}{l} \sqrt{\frac{3al_f}{4\pi}} r(x) \\ &= \sqrt{\frac{3\alpha x(1-x)m^2}{4pL}} r(x). \end{aligned}$$

Note that the emission probability is proportional to $r(x)$, indicating that the radiating electron does not flip helicity. The classical LP result in the limit of $(1/6)al_f b_l \gg 1$ is

$$\frac{(1-x)}{l} \frac{dP_{LP}(x)}{dx} = \frac{\sqrt{2}}{3} \sqrt{\frac{3\alpha(l-x)m^2}{4pL}}, \quad (9.8)$$

which is smaller than our result, Eq. (9.7), by a factor of 0.471 for x near one. The calculation by Migdal, the LPM effect, yields the result

$$\frac{(1-x)}{l} \frac{dP_{LPM}(x)}{dx} = 2 \sqrt{\frac{2}{3\pi}} \sqrt{\frac{3\alpha x(1-x)m^2}{4pL}} r(x), \quad (9.9)$$

when his approximate formulas are normalized to the correct result in the Bethe-Heitler limit. Equation (9.9) is roughly 8% smaller than Eq. (9.7).

B. Finite target

All the regions of integration must be evaluated explicitly for the case of a target of finite thickness. The full expression is written in a form suitable for numerical integration:

$$I(\text{tot}) = I(0-) + I(+0) + I(00) + I(+ -), \quad (9.10)$$

where

$$I(0-) = I(+0) = \left[\int_0^{b_l} db \int_0^b db_2 + \int_{b_l}^{\infty} db \int_0^{b_l} db_2 \right] \frac{2C(b)}{b} \left\{ \left(1 + \frac{1}{2} r(x) al_f b_2 \right) \sin\left(b + \frac{1}{6} al_f \frac{b_2^2}{b} (3b - 2b_2)\right) - \sin[b] \right\}, \quad (9.11)$$

$$I(+ -) = \int_{b_l}^{\infty} db \int_{b_l}^b db_2 \frac{2C(b)}{b} \left\{ \left(1 + \frac{1}{2} r(x) al_f b_l \right) \sin\left(b + \frac{1}{6} al_f \frac{b_l}{b} P(b, b_2)\right) - \sin[b] \right\},$$

where

$$P(b, b_2) = b_l(3b - 2b_l) + 6(b_2 - b_l)(b - b_2), \quad (9.12)$$

and $I(00)$ is given in Eq. (9.6).

In the BH and the soft-photon limit, $x \rightarrow 1$, it has already been shown that

$$I(\text{BH}) = \frac{2}{3} al_f b_l = \frac{2}{3} al. \quad (9.13)$$

Therefore it is natural to introduce a form factor F and two scaling variables that track the LPM effect by defining

$$I(\text{tot}) = I(\text{BH})F(N, T, x), \quad (9.14)$$

where the x dependence arises only from the spin factor $r(x)$, $N = (1/6)al_f$ is essentially the number of formation lengths contained in a mean free path, and T is the thickness of the target in units of the mean free path, i.e.,

$$T = Nb_l = \frac{\pi}{3} \frac{l}{\alpha L} \quad \text{with} \quad N = \frac{1}{6} al_f = \frac{\pi}{3} \frac{l_f}{\alpha L}. \quad (9.15)$$

The form factor F will be divided into separate contributing regions as was the integral I . Inserting the scaling variables into Eqs. (9.12) and (9.6) and recalling the relation $b_l = T/N$ then leads to

$$F(0-) = F(+0) = \left[\int_0^{b_1} db \int_0^b db_2 + \int_{b_1}^{\infty} db \int_0^{b_1} db_2 \right] \frac{C(b)}{2Tb} \left\{ [1 + 3r(x)Nb_2] \sin \left(b + N \frac{b_2^2}{b} (3b - 2b_2) \right) - \sin[b] \right\}, \quad (9.16)$$

$$F(+ -) = \int_{b_1}^{\infty} db \int_{b_1}^b db_2 \frac{C(b)}{2Tb} \left\{ [1 + 3r(x)T] \sin \left(b + T \frac{1}{b} P(b, b_2) \right) - \sin[b] \right\},$$

where

$$P(b, b_2) = b_1(3b - 2b_1) + 6(b_2 - b_1)(b - b_2), \quad (9.17)$$

and finally

$$F(00) = \int_0^{b_1} db \frac{C(b)}{2Tb} (b_1 - b) \{ [1 + 3r(x)Nb] \sin[b + Nb^2] - \sin[b] \}. \quad (9.18)$$

These contributions to the form factor cannot be interpreted as radiation from the surfaces, from the exterior, and from the interior of the target, respectively, because the contributions from each region is not positive definite. The total sum, the form factor F , is positive definite.

Note that in the BH limit of small T , $F \rightarrow 1$, the defined normalization. In the LPM limit of $T \gg N \gg 1$, which ensures that $b_1 = T/N$ is also much larger than one, the form factor can be shown to be dominated by $F(00)$. One then finds $F \rightarrow (3/4)r(x)\sqrt{\pi/2N}$. Since N is proportional to $(1-x)^{-1}$, the form factor F vanishes as the square root of k in the soft-photon limit. This is the expected suppression from the LPM effect.

X. PHYSICAL INTERPRETATION AND NUMERICAL RESULTS

In this section we discuss and illustrate the physical phenomena that are reflected in the behavior of the form factor $F(N, T, x)$ as a function of the scaling variables T and N . First, recall the definitions of the scaling variables:

$$T = \frac{\pi}{3} \frac{l}{\alpha L}, \quad N = \frac{\pi}{3} \frac{l_f}{\alpha L},$$

$$b_1 = \frac{l}{l_f}, \quad l_f = \frac{2xp}{m^2(1-x)} = \frac{2p_i p_f}{m^2 k}. \quad (10.1)$$

The behavior of the form factor in certain limiting regimes is quite easy to interpret physically. Keep in mind that T is determined by the target geometry and composition, not kinematics. On the other hand, the value of N is determined by kinematics and target composition, not target geometry; N increases as the photon energy k decreases.

Small T : In this regime, the target thickness is much less than the mean free path. Thus there can be little multiple scattering and the form factor must be close to 1, signifying the predominance of the Bethe-Heitler process. For $N \ll T$, the value of the form factor F is controlled by the integration region (00). Contributions from the exterior regions grow for larger N values. Eventually, the double exterior region (+ -) dominates.

Large T : The target thickness is much greater than the mean free path. Thus the electron will definitely undergo many multiple-scattering events in traversing the target. The form-factor behavior and its physical interpretation depend strongly upon the value of N . For N much smaller than 1, that is for $l_f \ll \alpha L$, the quadratic-phase oscillation is negligible, the region (00) dominates, and $F \sim 1$; the physics is that of the Bethe-Heitler process. For larger N in the region $T \gg N \gg 1$, the quadratic-phase oscillation is important and it controls the value of $F(00)$. This is the LPM regime in which the form factor asymptotically varies as $N^{-1/2}$, the characteristic of LPM suppression of bremsstrahlung. For even larger N in the region $N \gg T \gg 1$, the formation length is larger than the large target thickness. The LPM suppression is incomplete in that the multiple scattering only takes place over a

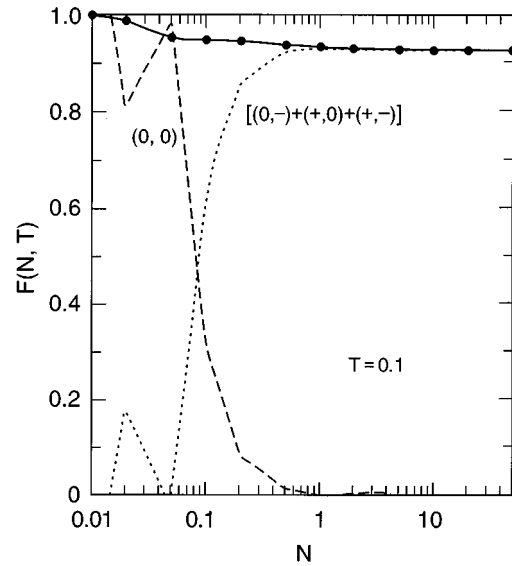


FIG. 1. A plot of the form factor $F(N, T)$ at $T=0.1$, that is, the target thickness is one-tenth of the radiation length, for a range of N values. The solid curve is the total form factor. The dashed curve labeled (00) is the contribution from inside the target. The dotted curve is the contribution when at least one source coordinate is outside the target. The curves are computed only at the indicated points and connected by straight lines.

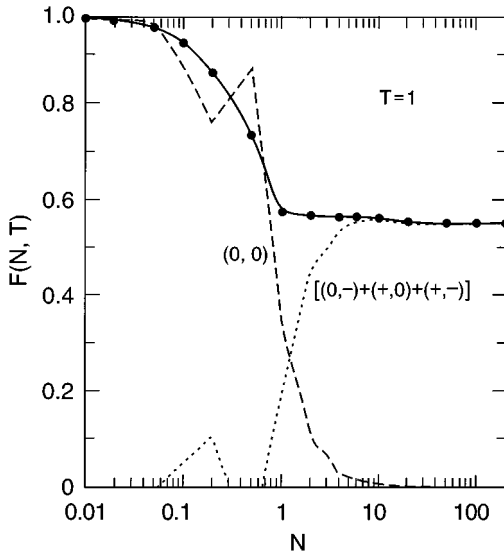


FIG. 2. A plot of the form factor $F(N, T)$ at $T=1.0$, that is, the target thickness is equal to one radiation length. The various curves are described in the caption to Fig. 1.

fraction of the formation length. The integration region (00) contributes less to the form factor F , and the mixed regions (0-), (+0), and (+-) eventually become the dominant contributors as N increases further into the region $N > T^2$.

The behavior discussed above can be directly seen in the numerical evaluation of the form factor [18]. All calculations were done in the soft-photon limit $r(x) \sim 1$.

It is found that $F(N, T=0.01) \approx 1$ for all N . As N varies from 0.001 up to 10, that is for $10 > b_l > 0.001$, the form factor decreases very slightly, less than 1 percent. For $N \leq T$, the (00) region dominates, while for larger values the exterior regions dominate.

In Figs. 1-3, the form factor $F(N, T)$ is plotted as a function of N for selected T values in the experimental range of

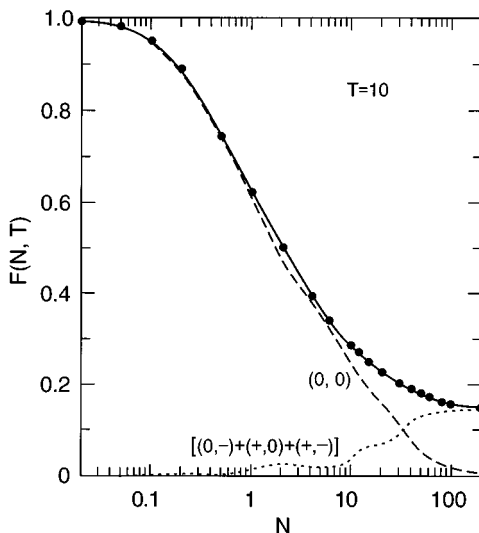


FIG. 3. A plot of the form factor $F(N, T)$ at $T=10$, that is, the target thickness is ten times the radiation length. The various curves are described in the caption to Fig. 1.

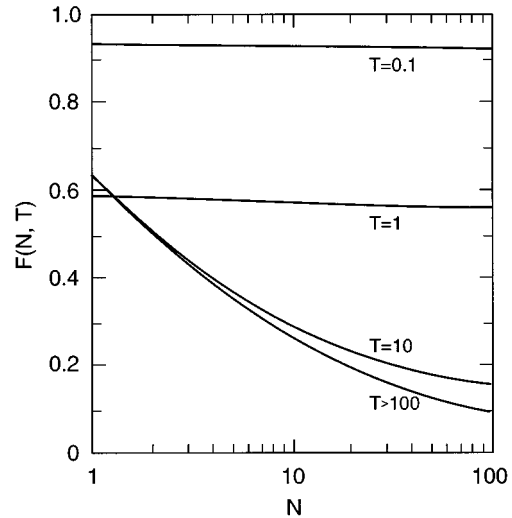


FIG. 4. A plot of the form factor $F(N, T)$ for a range of T values is plotted against N . The important dependence on the target thickness and the approach to the thick target limit of LPM is evident.

interest. The computer data are not smoothed and the curves are composed of straight-line segments connecting the computed points. The dashed lines show the contribution of the purely internal region (00). The dotted lines arise from the remaining mixed and external regions, $[(0-)+(+,0)+(+-)]$. The total form factor always has an overall smooth behavior, but definite oscillatory contributions from the interior and external integration regions arise from the sinusoidal integrands. For $N \leq T$, the internal region dominates the form factor. For somewhat larger- N values, the external regions dominate.

In Fig. 1, $F(N, T=0.1)$ is plotted for N ranging from 0.01

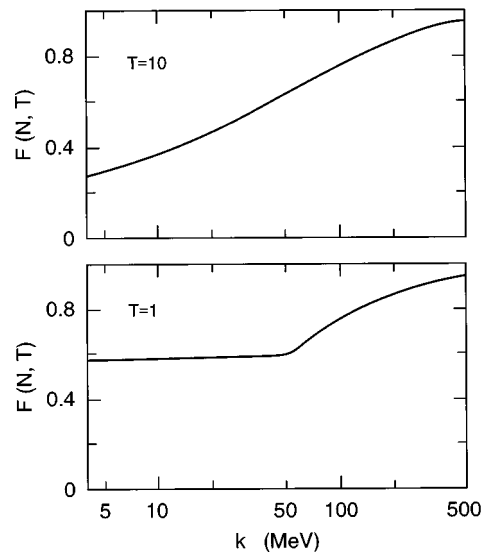


FIG. 5. Plots of the form factor $F(N, T)$ vs k for $T=10$ and 1 are given. The physical parameters were chosen to roughly correspond to the SLAC experiment for a gold target of thickness 6% L and 0.7% L , respectively. Note the break at $k \approx 50$ MeV in the $T=1$ data.

to 50, or b_l ranging from 10 down to 0.002. In Fig. 2 $F(N, T=1)$ is plotted for N ranging from 0.02 to 200 ($500 > b_l > 0.05$). In Fig. 3 the form factor $F(N, T=10)$ is plotted for N , again ranging from 0.02 to 200. The small-scale oscillations in the individual contributions are evident. The LPM regime is the region $1 < N \leq T$ where (asymptotically) the form factor should fall as $0.94/\sqrt{N}$. In all the graphs the regime $N \geq T^2$, in which the form factor becomes independent of N but T dependent, is evident. As N increases, one eventually enters into the regime of low-photon energies and the index of refraction of the medium becomes important. These effects are not treated here.

In Fig. 4 the form factor $F(N, T)$ for different T values is plotted against N . This plot shows the behavior as the target thickness increases from a thin target, $T=0.1$, to the very thick-target LPM limit, $T > 100$. Finally, in Fig. 5 the form factor $F(N, T)$ for two T values is plotted against the photon momentum k . We emphasize that this calculation assumed single-photon emission only. The values of $T=10$ and 1 approximately correspond to the SLAC experiment for a gold target of 6% L and 0.7% L , respectively. The break in the slope at $k=50$ MeV is an effect of finite-target thickness. This break is present in the data of [5] for a beam energy of 25 GeV (in which the radiation length L is denoted by X_0). For k values smaller than this value, the formation length becomes larger than the target thickness. Detailed comparisons of our results for finite target thickness and the experimental data are in preparation by the SLAC E-146 Collaboration.

Note added. After this work was submitted for publication, we became aware of three earlier papers which extended the classical treatment of the LPM effect [19–21]. In particular, the error in the treatment of Landau and Pomeranchuk discussed in the Appendix was first pointed out and corrected in [20].

ACKNOWLEDGMENTS

We thank Spencer Klein and Ralph Becker-Szendy for interesting discussions of the LPM effect and of the data taken by the SLAC E-146 collaboration. R.B. thanks Professor R. Sugar of the University of California at Santa Barbara for his hospitality and support during the initial stages of this work. S.D. thanks Professor N. Khuri and Professor T. D. Lee at Rockefeller and Columbia Universities, respectively, for their hospitality and support during the spring of 1995 while this work was being completed. This work was supported by U.S. Department of Energy Contract No. DE-AC03-76SF00515.

APPENDIX

In this appendix we show the error in the Landau-Pomeranchuk classical derivation that led them to choose $\langle \vec{p}_\perp^2 \rangle = 4\pi m^2/\alpha$ in order to get the correct Bethe-Heitler limit instead of (8.6). Our starting point is Eq. (1) in Sec. 76 entitled “Electron-Cascade Processes at Ultra-High Energies,” in the collected works of [8]. If the higher-order terms in $1/g$ are *not* neglected, where $g \equiv \omega r_{12}$ with $\vec{r}_{12} = \vec{r}_1 - \vec{r}_2$,

one finds, in place of their Eq. (2), the result

$$dI = dI_1 + dI_2,$$

where

$$dI_i = \frac{e^2 \omega d\omega}{\pi} \int_{-\infty}^{\infty} \int dt_1 dt_2 \frac{\exp[i\omega(t_1 - t_2)]}{r_{12}} J_i. \quad (\text{A1})$$

The integrands are

$$\begin{aligned} J_1 &= \left[\vec{V}_1 \cdot \vec{V}_2 - \frac{(\vec{V}_1 \cdot \vec{r}_{12})(\vec{V}_2 \cdot \vec{r}_{12})}{r_{12}^2} \right] \\ &\times \left[\sin(g) + 3 \frac{g \cos(g) - \sin(g)}{g^2} \right], \\ J_2 &= [-2 \vec{V}_1 \cdot \vec{V}_2] \left[\frac{g \cos(g) - \sin(g)}{g^2} \right]. \end{aligned} \quad (\text{A2})$$

The leading contributions to these integrals comes from the slowly oscillating terms with phase $\omega[(t_1 - t_2) - r_{12}]$. That is, when $\omega(1 - V)(t_1 - t_2) \leq 1$, where V is the velocity. In this case $g \sim (1 - V)^{-1} \gg 1$.

This argument led Landau and Pomeranchuk to neglect all terms of order $1/g^2$. Although this approximation is valid for the second term in J_1 , it is invalid for J_2 , which has a coefficient $\vec{V}_1 \cdot \vec{V}_2 \sim 1$ in contrast to the coefficient in J_1 that vanishes in the limit of small scattering.

To be specific, consider a single scattering (classical) at $t=0$ so that we can write, to order $|\Delta V|^2 \ll 1$,

$$\vec{V}(t) = \vec{V}(0) \left[1 - \frac{1}{2} \frac{|\Delta V|^2}{V(0)^2} \theta(t) \right] + \Delta \vec{V} \theta(t), \quad \vec{V}(0) \cdot \Delta \vec{V} = 0. \quad (\text{A3})$$

Defining $\theta_i = \theta(t_i)$, we find

$$\begin{aligned} \vec{V}_1 \cdot \vec{V}_2 &= V(0)^2 \left[1 - \frac{1}{2} \frac{|\Delta V|^2}{V(0)^2} (\theta_1 - \theta_2)^2 \right], \\ g &= \omega V(0)(t_1 - t_2) \left[1 + \frac{1}{2} \frac{|\Delta V|^2}{V(0)^2} \frac{t_1 t_2}{(t_1 - t_2)} (\theta_1 - \theta_2)^2 \right], \\ \vec{V}_1 \cdot \vec{V}_2 - \frac{(\vec{V}_1 \cdot \vec{r}_{12})(\vec{V}_2 \cdot \vec{r}_{12})}{r_{12}^2} &= |\Delta V|^2 \frac{t_1 t_2}{(t_1 - t_2)^2} (\theta_1 - \theta_2)^2. \end{aligned} \quad (\text{A4})$$

The Landau-Pomeranchuk result is I_1 , which can be readily evaluated as

$$dI_1 = \frac{e^2 E^2 |\Delta V|^2}{3\pi m^2} d\omega = \frac{e^2 |\Delta p|^2}{3\pi m^2} d\omega, \quad (\text{A5})$$

which is precisely 1/2 the correct classical answer. Next, one readily finds that the integral I_2 is also, to leading order, proportional to $|\Delta p|^2/m^2$ with the contribution coming from the term in g proportional to ΔV^2 . The result is that $I_1 = I_2$ which accounts for the missing contribution.

- [1] H. A. Bethe and W. Heitler, Proc. R. Soc. **A146**, 83 (1934).
- [2] S. R. Klein *et al.*, *A Measurement of the LPM Effect*, Proceedings, of the XVI International Symposium on Lepton and Photon Interactions, Ithaca, NY, 1993 (AIP, New York, 1994), p. 172.
- [3] SLAC E-146 Collaboration, R. Becker-Szendy *et al.*, Quantum Mechanical Suppression of Bremsstrahlung, Proceedings of the SLAC Summer Institute, 1993 [SLAC Report No. 444 (unpublished)]; p. 519, in Proceedings of the XXIII International Symposium on Multiparticle Dynamics, Aspen, Co, 1993 (World Scientific, Singapore, 1994), pp. 527–541.
- [4] Martin L. Perl, *Notes on the Landau, Pomeranchuk, Migdal Effect: Experiment and Theory*, Proceedings of the Results and Perspectives in Particle Physics, 1994 (Editions Frontieres, Gif-sur-Yvette, France, 1994), p. 753.
- [5] P. Anthony *et al.*, Phys. Rev. Lett. **75**, 1949 (1995).
- [6] R. Blankenbecler and S. D. Drell, Phys. Rev. D **36**, 277 (1987). An extensive list of earlier references are given here.
- [7] R. Blankenbecler and S. D. Drell, “A Quantum Treatment of the Landau-Pomeranchuk-Migdal Effect,” SLAC Report No. SLAC-PUB-95-6875 (unpublished).
- [8] L. D. Landau and I. J. Pomeranchuk, Dokl. Akad. Nauk. SSSR **92**, 535 (1953); **92**, 735 (1953). See also L. Landau, *The Collected Papers of L. D. Landau* (Pergamon, New York, 1965), Secs. 75–76, pp. 586–593.
- [9] A. B. Migdal, Phys. Rev. **103**, 1811 (1956).
- [10] See, for example, E. L. Feinberg and I. J. Pomeranchuk, Nuovo Cimento **3**, 652 (1956); J. S. Bell, Nucl. Phys. **8**, 613 (1958).
- [11] M. Gyulassy and X.-N. Wang, Nucl. Phys. **B420**, 583 (1994); X.-N. Wang, M. Gyulassy, and M. Plümer, Phys. Rev. D **51**, 3236 (1995).
- [12] Photon and gluon emission in an infinite medium are described in R. Baier, Yu. L. Dokshitser, S. Peigne, and D. Schiff, Phys. Lett. B **345**, 277 (1995).
- [13] V. M. Galitsky and I. I. Gurevich, Il Nuovo Cimento **32**, 396 (1964).
- [14] Bruno Rossi, *High-Energy Particles* (Prentice-Hall, New York, 1952), see, in particular, Chap. 2.
- [15] Contributions due to electron spin are included later. Since contributions of order $1/p$ need to be retained only in the phase of the electron wave function, not the current operator, spin effects can be incorporated very simply.
- [16] The index of refraction of the medium can be included in the photon wave function at this juncture. However, it will be neglected in the present treatment. Its effects have been discussed in the papers in [10].
- [17] D. V. Schreorder, “Beamstrahlung and QED Backgrounds at Future Linear Colliders,” SLAC Report No. 371, 1990 (unpublished), see especially, Sec. 4.4, Eq. (4.84).
- [18] For numerical simplicity the cutoff function was chosen to be
- $$C(z)=\exp[-\epsilon|z|] \quad (-\infty < z < 0),$$
- $$C(z)=1 \quad (0 < z < l),$$
- and $C(z)=\exp[-\epsilon(z-l)] \quad (l < z < \infty)$.
- The numerical results are insensitive to the value of ϵ .
- [19] N. F. Shul’ga and S. P. Fomin, JETP Lett. **27**, 117 (1978).
- [20] A. I. Akhiezer and N. F. Shul’ga, Sov. Phys. Usp. **25**, 541 (1982).
- [21] N. V. Laskin, A. S. Mazmanishvili, N. N. Nasonov, and N. F. Shul’ga, JETP Lett. **62**, 438 (1985).